Theoretical and Experimental Studies on the Adsorption of Aromatic Compounds onto Cellulose

5 AUTHORS, INCLUDING:

Denilson Da Silva Perez
FCBA Institut Technologique
90 PUBLICATIONS **642** CITATIONS

SEE PROFILE

Reinaldo Ruggiero
Universidade Federal de Uberlândia (UFU)
51 PUBLICATIONS **691** CITATIONS

SEE PROFILE

Antonio Eduardo Da Hora Machado
Universidade Federal de Uberlândia (UFU)
116 PUBLICATIONS **1,152** CITATIONS

SEE PROFILE

Karim Mazeau
University Joseph Fourier - Grenoble 1
93 PUBLICATIONS **1,993** CITATIONS

SEE PROFILE

Theoretical and Experimental Studies on the Adsorption of Aromatic Compounds onto Cellulose

Denilson Da Silva Perez,*,[†,‡,§] Reinaldo Ruggiero,[‡] Luis C. Morais,[‡]
Antônio E. H. Machado,[‡] and Karim Mazeau[†]

Centre de Recherches sur les Macromolécules Végétales (CERMAV−CNRS), affiliated with University Joseph Fourier BP 53, 38041, Grenoble Cedex 9, France, and Instituto de Quimica, Universidade Federal de Uberlândia, P.O. Box 593, 38400-902, Uberlândia, MG, Brazil

Received September 24, 2003. In Final Form: January 13, 2004

The adsorption of several aromatic compounds over microcrystalline cellulose was studied by molecular modeling and experimentally using gas chromatography. Experimental adsorption enthalpies were obtained from an equation based on Clausius−Clapeyron formalism and the temperature dependence of retention volume at infinite dilution. Four different cellulose surfaces (three crystalline (110, 100, and 010) and one amorphous) were modeled. Overall strong agreement was observed between the experimental and theoretical work with 84% of the adsorbate−cellulose systems having differences between measured and predicted values of less than 20%. Based on both calculated and experimental data, a morphology for the microcrystalline cellulose as a weighted combination of the four surfaces was proposed: 39% (110), 28% (100), 10% (010), and 23% amorphous. By adopting this distribution, differences between experimental and weighted average predicted adsorption energies were 10% or less for 14 out of 17 compounds; a maximum of 15% was observed for guaiacol. Experimental results for monosubstituted aromatic compounds revealed that adsorption enthalpies are related to the hydrophilic/hydrophobic character of the substituent groups: 3.5 kJ mol^{-1} for a methyl group, 15.7 kJ mol^{-1} for a double bond, 21.0 kJ mol^{-1} for a methoxyl group, 22.8 kJ mol^{-1} for a carbonyl group, and 27.6 kJ mol^{-1} for a hydroxyl group. These tendencies were confirmed by modeling, except for the aldehyde carbonyl group, where an overestimation of 10.8 kJ mol^{-1} was observed. Analysis of experimental and predicted adsorption enthalpies of multisubstituted aromatic compounds suggests that the efficiency of their interaction with cellulose depends on a compromise between the roughness of the cellulose surface and their conformational adaptability.

Introduction

Cellulose, the most abundant natural polymer in nature, occurs mainly in association with other polysaccharides (hemicelluloses) and the aromatic macromolecule lignin. The interactions between these components at a molecular level are not well-established whether they occur in the vegetal or in cellulosic pulps for papermaking.[1] An improved understanding would allow a deeper comprehension of the structure and dynamics of plant cell walls, the optimization of industrial processes, or even the design of novel biomimetic materials.

The existence of chemical linkages between lignin and some hemicellulose fragments that form lignin−polysaccharide complexes (LPCs) is well accepted,[2−5] but the interactions between cellulose and lignin seem to be based only on physical forces. Two main types of interactions should be considered: electrostatics, in particular hydrogen bonds, caused by phenolic and alcoholic hydroxyl groups (that can act as donators or receptors) and carbonyl, methoxyl groups, or even σ-rich bases and weaker associations, resulting from van der Waals interactions along the macromolecular association of the wood components.[1]

A useful experimental tool for understanding such interactions is the study of adsorption of probe compounds over the surface of cellulosic materials by gas chromatography.[6−13] Thermodynamical data of the adsorption of carefully selected compounds on cellulose can reveal its capacity for interaction, providing important information for understanding the adsorption process.

A simple, rapid, and accurate method to get thermodynamic measurements is based on Henry's law and requires the determination of temperature dependence of retention volume at infinite dilution using a mathematical model based on Clausius−Clapeyron's equation.[14−17]

Gray and co-workers have studied the adsorption of *n*-alkanes on pure cotton cellulose,[6,7] cellophane (regenerated cellulose),[10] and lignin-free kraft[8] and lignin-rich thermomechanical (TMP) pulps.[6,7] The three most important adsorption thermodynamic parameters (free energy, enthalpy, and entropy) were found to vary linearly

† Centre de Recherches sur les Macromolécules Végétales.
‡ Universidade Federal de Uberlândia.
§ Current address: AFOCEL, Wood Process Laboratory, Domaine de l'Etançon, 77370 Nangis, France.

(1) Fengel, D.; Wegener, G. *Wood: Chemistry, Ultrastructure, Reactions*; W. de Gruyter: Berlin, 1988.
(2) Hemmingson, J. A.; Leary, G. J.; Miller, I. J.; Thomas, W. A.; Woodhouse, A. D. *J. Chem. Soc., Chem. Commun.* **1978**, 92−93.
(3) Eriksson, O.; Goring, D. A. I.; Lindgren, B. O. *Wood Sci. Technol.* **1980**, *14*, 267−279.
(4) Gerasimowicz, W. V.; Hicks, K. B.; Pfeffer, P. E. *Macromolecules* **1984**, *17*, 2597−2603.
(5) Joseleau, J. P.; Kesraoui, R. *Holzforschung* **1986**, *40*, 163−168.

(6) Dorris, G. M.; Gray, D. G. *J. Colloid Interface Sci.* **1979**, *71*, 93−106.
(7) Dorris, G. M.; Gray, D. G. *J. Colloid Interface Sci.* **1980**, *77*, 353−362.
(8) Gurnagul, N.; Gray, D. G. *Can. J. Chem.* **1987**, *65*, 1935−1939.
(9) Katz, S.; Gray, D. G. *J. Colloid Interface Sci.* **1981**, *82*, 339−351.
(10) Katz, S.; Gray, D. G. *J. Colloid Interface Sci.* **1981**, *82*, 326−338.
(11) Dernovaya, L. A.; Eltekov, Y. A.; Hradil, J.; Svec, F. *J. Chromatogr.* **1991**, *552*, 365−370.
(12) Belgacem, M. N.; Blayo, A.; Gandini, A. *J. Colloid Interface Sci.* **1996**, *182*, 431−436.
(13) Zou, G. W.; Zheng, Q.; Shao, Y.; Hu, G. J. *Chromatographia* **1996**, *42*, 462−464.
(14) Neumann, M. G. *J. Chem. Educ.* **1976**, *53*, 708−710.
(15) Atkinson, D.; Curthoys, G. *J. Chem. Educ.* **1978**, *55*, 564−566.
(16) Bruner, F.; Ciccioli, P.; Brancaleoni, E.; Longo, A. *Chromatographia* **1975**, *8*, 503−506.
(17) Ruggiero, R.; De Groote, R. A. M. C.; Neumann, M. G. *J. Chromatogr.* **1984**, *285*, 182−187.

with the number of carbon atoms in the alkane chain. Some differences in values were obtained as a function of purity (bleached or lignin-rich pulps), crystallinity and polymorphism (cellulose II for cellophane and cellulose I for others), and fiber morphology and organization (unbeaten and beaten fibers and paper). The London nonpolar component of surface free energy was found to vary from 38.8 (thermomechanical pulps) to 49.9 mM m^{-1} (cotton cellulose). The proximity of the adsorption enthalpies of the studied *n*-alkanes and their respective heat of liquefaction indicates that the adsorption takes place by means of weak interactions.

Dernovaya and collaborators[11] studied the interaction between cellulose and a set of polar probes. They observed strong interactions between the cellulose surface and the polar moieties of the probe compounds through the formation of hydrogen bonds, as revealed by enthalpy data. The authors showed that cellulose presents a polarity superior to that of known sorbents such as Chromosorb 104, Polysorb N, and Synachrome E5. The strong polar behavior of cellulose has been confirmed by Spange and co-workers. Using a solvatochromic technique,[18] the authors established that cellulose presents a Gutmann's acceptor number that is higher than that of aliphatic alcohols such as ethanol and methanol.

Molecular modeling has become a powerful tool for the study of multicomponent macromolecular systems providing atomistic details of association and precise indications of the interactions stabilizing the complexes. However, to study the adsorption process on cellulose materials by means of molecular modeling, a realistic atomistic description of their surfaces is crucial.

The basic structural element of all native cellulose is the crystalline microfibril, where a number of long cellulose chains are tightly packed in a parallel, nearly perfect way. Depending on the sample origin, the number of chains in a given microfibril ranges from about 20 in the primary wall cellulose to more than 1000 in the secondary wall of some green algae such as Valonia or in tunicates.[19] The morphological features of the largest cellulose microfibrils have been described by transmission electron microscopy (TEM) using the diffraction contrast modes. Roughly, the cross section of these microfibrils shows a parallelogram shape, with angles close to 90° for Valonia[20,21] and sharp acute (55°) or obtuse angles (125°) in the case of tunicin and the tunicate cellulose, respectively.[22,23] In both cases eroded corners are observed, more frequently for tunicin than for Valonia.

In this work, we have only considered the cellulose Iβ allomorph. Although the allomorph Iα has different space group and unit cell parameters, the exposed surfaces of a given microfibril have essentially the same molecular geometry as that of cellulose Iβ. In Valonia, the sides of the section correspond to the (110) and (1$-$10) cellulose planes. In tunicin, the eroded corners reveal the (010) and the (100) planes.[23] TEM observations of Valonia microfibrils have been corroborated by atomic force microscopy (AFM) work that showed surface cellulose
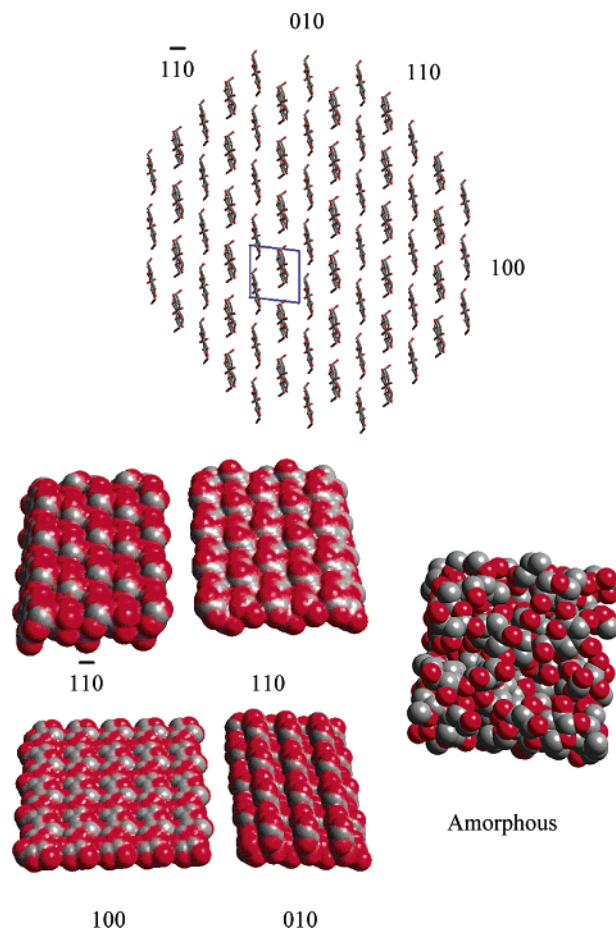

Figure 1. Cross section of the cellulose Iβ crystal phase in a view parallel to the helical axis. The four principal cleavage planes are labeled by their Miller indices. The corresponding organized surfaces viewed perpendicular to the fiber axis and the amorphous surface are all reported.

chains in perfect register.[19,24] In addition, the existence of an exposed surface (100) could also be inferred from several gold-covered cellulose binding modules (CBM) adsorbed at the corner of Valonia microfibrils where this face is located.[25]

Figure 1 is a schematic representation of the molecular cross section of a crystalline cellulose microfibril perpendicular to the microfibril axis. It corresponds to a truncated parallelogram, revealing the four exposed planes: (110), (1$-$10), (010), and (100). In the same figure, the four corresponding surfaces seen along the cellulose chain axes are given. An amorphous phase is also represented. The surface roughness, the density of surface groups, and their polarity are shown in Figure 1.

Several studies have dealt with the interaction of cellulose surfaces with small molecules. The adsorption of water[26$-$28] and lignin oligomers[29] on only the crystalline surfaces (110) and (1$-$10) have been reported. In a recent study,[30] we characterized the atomic details of the

(18) Spange, S.; Heinze, T.; Klemm, D. *Polym. Bull.* (*Berlin, Germany*) **1992**, *28*, 697$-$702.
(19) Bayer, E. A.; Chanzy, H.; Lamed, R.; Shoham, Y. *Curr. Opin. Struct. Biol.* **1998**, *8*, 548$-$557.
(20) Sugiyama, J.; Harada, H.; Fujiyoshi, Y.; Uyeda, N. *Planta* **1985**, *166*, 161$-$168.
(21) Revol, J. F. *Carbohydr. Polym.* **1982**, *2*, 123$-$134.
(22) Revol, J.-F.; Daele, Y. V.; Gaill, F.; Goffinet, G. *Biol. Cell.* **1992**, *76*, 87$-$96.
(23) Helbert, W.; Nishiyama, Y.; Okano, T.; Sugiyama, J. *J. Struct. Biol.* **1998**, *124*, 42$-$50.

(24) Baker, A. A.; Helbert, W.; Sugiyama, J.; Miles, M. J. *Biophys. J.* **2000**, *79*, 1139$-$1145.
(25) Lehtio, J.; Sugiyama, J.; Gustavsson, M.; Fransson, L.; Linder, M.; Teeri, T. T. *Proc. Natl. Acad. Sci. U.S.A.* **2003**, *100*, 484$-$489.
(26) Biermann, O.; Hadicke, E.; Koltzenburg, S.; Muller-Plathe, F. *Angew. Chem., Int. Ed.* **2001**, *40*, 3822$-$3825.
(27) Heiner, A. P.; Teleman, O. *Langmuir* **1997**, *13*, 511$-$518.
(28) Heiner, A. P.; Kuutti, L.; Teleman, O. *Carbohydr. Res.* **1998**, *306*, 205$-$220.
(29) Houtman, C. J.; Atalla, R. H. *Plant Physiol.* **1995**, *107*, 977$-$984.
(30) Mazeau, K.; Vergelati, C. *Langmuir* **2002**, *18*, 1919$-$1927.

interaction of benzophenone on the (110), (1−10), and (100) crystalline and one amorphous surfaces of cellulose. In that work, a benzophenone monolayer was deposited on each surface and the geometrical and energetic dependences of the adsorption parameters were calculated with respect to the surface characteristics. Both the geometry of the adsorption and the energetic component stabilizing the complex were found to depend on the particular geometry of the surfaces. Benzophenone adsorbs flat on the (100) surface, where many adsorption sites together with a great geometrical freedom were available. As expected, the adsorption on this surface resulted essentially from van der Waals interaction. A comparison of the adsorption on (110) and (1−10) surfaces shows no significant difference regarding the adsorption phenomenon. On both surfaces, the adsorption sites were better defined because they depend on the hydrogen bonds formed between the hydroxyl groups of cellulose and the carbonyl moiety of benzophenone. Therefore, these interactions could be defined as electrostatic. Finally, the adsorption geometry of benzophenone on amorphous cellulose surfaces was disordered, with the system being stabilized simultaneously by electrostatic and van der Waals interactions. Calculated data qualitatively agreed with independent adsorption experiments demonstrating that good confidence can be expected from our modeling methodology for the study of interfacial phenomena involving cellulose.

To our knowledge, the adsorption enthalpies of aromatic compounds on cellulose have been neither experimentally nor theoretically determined in detail. In this paper, we have determined the adsorption enthalpy of a series of aromatic compounds related to lignin, using these two complementary approaches. Experiments were based on gas chromatography under infinite dilution conditions, while atomistic simulations were achieved by combining molecular dynamics and energy minimization performed on a complex macromolecular system that mimics gas adsorption on a solid surface. From these studies, a comprehensive understanding of the adsorption process of substituted aromatic rings onto cellulose could be established.

Experimental Section

Experimental Adsorption Energy Measurements. A chromatographic column (2 m × 3.2 mm stainless steel) was packed with microcrystalline cellulose (60−100 mesh) and conditioned at 200 °C for 3 h under nitrogen. Thermogravimetric[31] and X-ray[32] diffraction studies have shown that crystalline cellulose is stable at this temperature under an inert atmosphere. The column was kept at 110 °C for 72 h prior to commencing experiments in order to remove residual moisture. During this study, cellulose was tested before and after packing for chemical and crystalline stability. Retention times of benzene and phenol were periodically checked during the work, and no significant differences were detected. Nevertheless, a slight yellowing of cellulose was observed at the end of the work, as expected owing to the thermal yellowing of cellulose.

All the compounds were dissolved in cyclohexane (10^{-3} M) prior to elution, and 2 μL of the solution was used for each injection. For benzene, 10 μL of vapor was injected because its retention time was very close to that of cyclohexane. All chemicals (P.A. grade) were purchased from Aldrich or Merck and used without further purification.

Elutions were carried out on a GC-14/A gas chromatograph equipped with FID detector and CR-6/A recorder (Shimadzu, Japan). The carrier gas was nitrogen, while hydrogen and synthetic air (nitrogen/oxygen mixture) was the flame gas. All

gases were Ultrapure grade (up to 99.99%). The carrier gas pressure was fixed at 5 Kgf/cm^2 for all experiments. Both injector and detector were kept at 250 °C. The column temperature varied from 110 to 160 °C, depending on the compounds, except for benzene, where the temperature range was 40−70 °C.

The injection dead time can be obtained from the elution time of a compound not interacting with the column, usually a gas such as methane. In this work, all the compounds were dissolved in cyclohexane (concentration ∼ 10^{-4} M) to facilitate the injection as well as to guarantee Henry's zero coverage hypothesis.

Peak symmetry was checked for the lowest temperature of elution for all the compounds. In the case of asymmetry of the peak, the temperature of elution was increased until satisfactory symmetric peaks were obtained. The retention volumes were not corrected for a possible pressure drop along the column.

The retention time of cyclohexane was found to be constant for temperatures higher than 110 °C. Apart from benzene, all the elution temperatures for aromatic compounds were over 110 °C; therefore it is reasonable to adopt the retention time of cyclohexane obtained for each run as the column dead time.

Molecular Modeling. *Modeled Systems.* Models of cellulose surfaces used in this study are based on a previous study on the atomistic understanding of benzophenone adsorption on cellulose.[30] A typical modeled system consists of a 3D periodic parallelepiped having at the bottom several layers of cellulose chains in their native crystalline or amorphous forms. The dimension of the parallelepiped perpendicular to the cellulose surface is deliberately enlarged to create an empty space above the molecular surface. However, some changes were introduced for the present study in order to improve the realism of the modeling. First, initial coordinates of the crystalline Iβ phase from crystallographic refinement of synchrotron X-ray and neutron diffraction data were used.[33] Then the surface chains of cellulose were allowed to be conformationally free (in the previous study they were partially constrained). Finally, a total of four different surfaces were considered instead of three previously. Three are crystalline, corresponding to the (110), (100), and (010) crystallographic planes of the cellulose Iβ allomorph, and the fourth is an amorphous surface.

Computational Details. Energy calculations were carried out by using the second-generation force-field PCFF specially suited for polymers and other materials.[34−38] The PCFF force field is an improved version of the ab initio consistent force field (CFF91) with new functional groups. The CFF91 force field has been parametrized and validated using condensed phase properties in addition to various ab initio and empirical data for molecules in isolation. The bound terms of the potential energy function include a quadratic polynomial for both bond stretching and angle bending, a three-term Fourier expansion for torsions and a Wilson out-of-plane coordinate term. Six cross terms up to the 3rd order are present to account for coupling between the intramolecular coordinates. The final two nonbonded terms use a Coulombic form for the electrostatic energy, and an inverse 6−9th power Lennard-Jones function is used for the van der Waals term. For the Coulombic term, the dielectric constant value was set to 1. All atoms are treated explicitly.

The process of minimization was performed by first the steepest descents and then the conjugated gradient method. The convergence criterion used was a root-mean-square (rms) force less than 0.1 (kcal/mol)/Å. Molecular dynamics simulation was then used in the NVT ensemble. The standard Verlet algorithm[39] was used to integrate Newton's law of motion with a time step of 0.001 ps. The molecular dynamics run was started by assigning

(31) Beckering, W. *J. Phys. Chem.* **1961**, *65*, 206−208.

(32) Martire, D. E.; Riedl, P. *J. Phys. Chem.* **1968**, *72*, 3478−3488.

(33) Nishiyama, Y.; Langan, P.; Chanzy, H. *J. Am. Chem. Soc.* **2002**, *124*, 9074−9082.

(34) Maple, J. R.; Dinur, U.; Hagler, A. T. *Proc. Natl. Acad. Sci. U.S.A.* **1988**, *85*, 5350−5354.

(35) Maple, J. R.; Hwang, M. J.; Stockfisch, T. P.; Dinur, U.; Waldman, M.; Ewig, C. S.; Hagler, A. T. *J. Comput. Chem.* **1994**, *15*, 162−182.
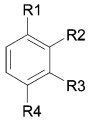
(36) Maple, J. R.; Hwang, M.-J.; Stockfisch, T. P.; Hagler, A. T. *Isr. J. Chem.* **1994**, *34*, 195−231.

(37) Sun, H.; Mumby, S. J.; Maple, J. R.; Hagler, A. T. *J. Am. Chem. Soc.* **1994**, *116*, 2978−2987.

(38) Sun, H. *Macromolecules* **1995**, *28*, 701−712.

(39) Verlet, L. *Phys. Rev.* **1967**, *159*, 98−103.

Table 1. Formulas of Aromatic Compounds Used as Adsorbate Probes

compound	R1	R2	R3	R4
acetophenone	(C=O)CH$_3$	H	H	H
anisole	OCH$_3$	H	H	H
benzaldehyde	CHO	H	H	H
benzene	H	H	H	H
benzyl alcohol	CH$_2$OH	H	H	H
cresol	OH	CH$_3$ (*o*)	H	H (*o*)
		H (*p*)		CH$_3$ (*p*)
1,2-dimethoxy-benzene	OCH$_3$	OCH$_3$	H	H
eugenol	OH	OCH$_3$	H	CH=CHCH$_3$
guaiacol	OH	OCH$_3$	H	H
isoeugenol	OH	OCH$_3$	H	CH$_2$CH=CH$_2$
phenol	OH	H	H	H
toluene	CH$_3$	H	H	H
xylene	CH$_3$	CH$_3$ (*o*)	CH$_3$ (*m*)	CH$_3$ (*p*)
		H (*m, p*)	H (*o, p*)	H (*o,m*)
styrene	CH=CH$_2$	H	H	H

the initial velocity for the atoms according to a Boltzmann distribution at $2T$, T being the target temperature. The velocities of the atoms were quickly scaled down so that the final temperature of atoms was T. Nose's algorithm[40] was used to keep the cell temperature constant.

Docking. The preferred adsorption sites are those where the interaction between an adsorbate (considered here as a guest molecule) and the molecular surface of cellulose is the most favorable, as revealed by combining molecular dynamics and energy minimizations. The guest molecule is initially placed within the computational box at 8–10 Å above the molecular surface. This distance is sufficient to allow the molecule to "feel" the surface and to progressively get closer to the surface, searching for the different adsorption sites. Fifty picoseconds of molecular dynamics is then performed at elevated temperature (600 K), the coordinates being saved each picosecond. The supermolecular arrangement having the lowest potential energy is then selected and fully minimized before another 30 ps of molecular dynamics at 500 K. Each of the 30 conformations of this dynamic run is minimized and saved for further analysis. The interaction energy is calculated as the difference between the total energy of the system and the sum of the energies of both isolated components (cellulose and guest molecule). Since the adsorption of 18 molecules on 4 cellulosic surfaces was studied, 72 systems were modeled, representing a total simulation time of 5.7 ns and 2160 energy minimizations.

To perform comparisons between predicted and experimental data, it was necessary to choose the most relevant value of the adsorption energy from the simulation. The experimentally observed adsorption enthalpies are in fact the averages of adsorbate–cellulose interactions occurring on different surfaces and geometries. Therefore, using all the interaction energy data from long molecular dynamics trajectories would be the best way to calculate an average value for the adsorption process. However, the large amount of computation needed to obtain statistical samples over 72 systems is beyond current computational power. Hence molecular dynamics has only been used to efficiently find the optimal adsorption sites, not to estimate interaction energies. The temperatures used are too high and the simulated time too short to be statistically meaningful. Such conditions allow the molecule to explore different adsorption sites. We have therefore considered the interaction energy as the average of 30 frames of the last molecular dynamic runs. All calculations were performed at the Centre d'Expérimentation et de Calcul Intensif, CECIC, Grenoble.

(40) Nosé, S. *Mol. Phys.* **1984**, *52*, 511–519.
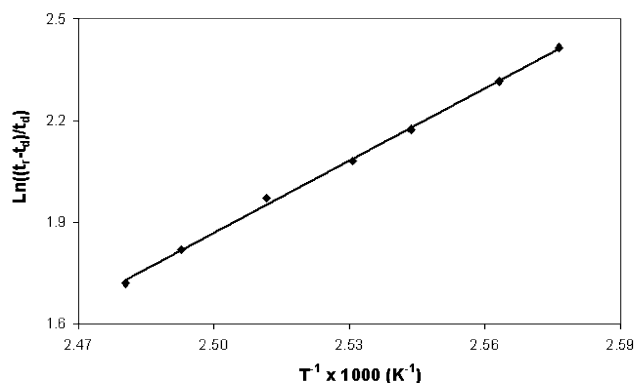
Figure 2. Temperature dependence of retention time of acetophenone eluting on a cellulose-packed chromatographic column. The adsorption energy is calculated from the slope according to eq 2.

Table 2. Adsorption Enthalpy at Infinite Dilution of the Studied Compounds over Cellulose and Their Heat of Condensation

adsorbate	$-\Delta H_{ads}$ (kJ mol^{-1})	$-\Delta H_{cond}$ (kJ mol^{-1})
acetophenone	59.4	48.9
anisole	57.7	43.5
benzaldehyde	59.5	48.5
benzene	36.7	33.8
benzyl alcohol	72.9	58.9
o-cresol	61.4	52.2
p-cresol	67.2	56.8
1,2-dimethoxybenzene	83.0	
eugenol	80.8	58.1
guaiacol	63.9	56.0
isoeugenol	84.8	58.9
phenol	64.3	49.7
toluene	39.8	35.9
xylene (*o, m, p*)	43.8	40.9–41.8
styrene	52.4	40.9

Results and Discussions

Experimentally Measured Adsorption Enthalpies. The Clausius–Clapeyron equation applied to adsorption takes the following form:

$$\frac{\partial \, \text{Ln} \, Kp}{\partial T} = \frac{\Delta H_{ads}}{RT^2} \qquad (1)$$

At infinite dilution condition, Kp can be replaced by the Henry's law constant, Ks,[6–8,10] which can be calculated from the corrected retention volume or retention time.[14–16] Therefore, the isosteric (i.e., all the interactions between the molecules of the adsorbate are neglected) adsorption enthalpy (ΔH_{ads}) can be obtained from

$$\text{Ln}\left(\frac{t_r - t_d}{t_d}\right) = \frac{\Delta H_{ads}}{RT} + C \qquad (2)$$

where t_r is the retention time of the substrate, t_d is the column dead time, and C is an integration constant.

The formulas of the aromatic compounds used in this study are depicted in Table 1. Adsorption enthalpies were determined from the linear regression of chromatographic data plotted according to eq 2. Linear correlation coefficients were observed to be higher than 0.99 for all the compounds. In Figure 2, the plot obtained for acetophenone is presented as an example. The experimental adsorption enthalpies and the heats of condensation are presented in Table 2.
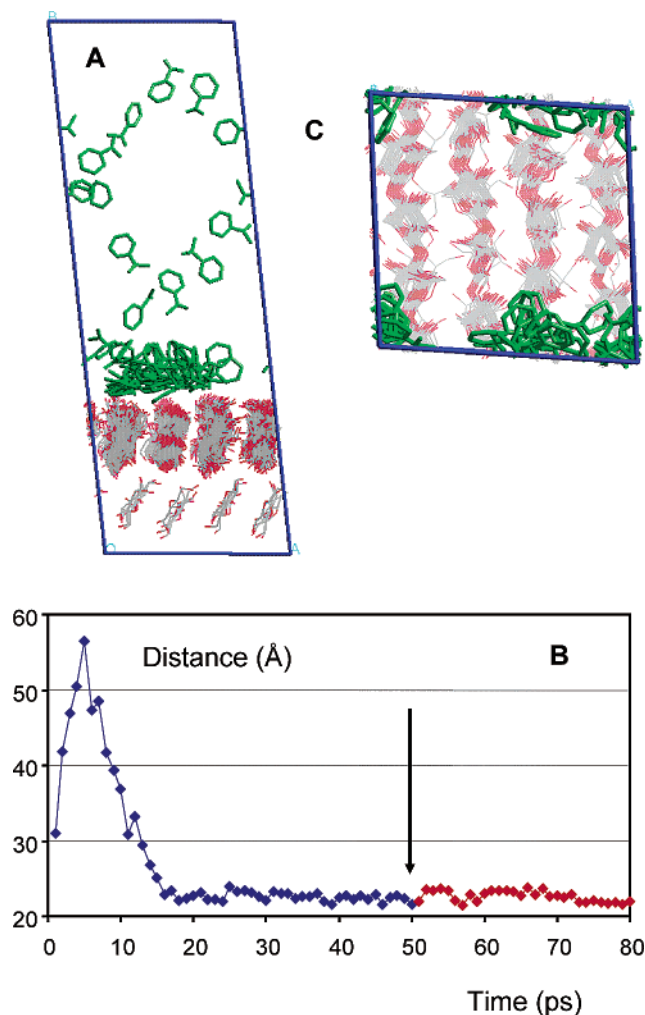
Figure 3. Illustration of the modeling procedure (the acetophenone molecule in the presence of the (110) surface of cellulose). (A) Superimposition of the 50 structures of the first molecular dynamics performed at elevated temperature (view parallel to the cellulose chain axis). (B) Time evolution of the distance between the guest molecule and the surface. (C) Superimposition of the final 30 structures of the second molecular dynamics at lower temperature (view perpendicular to the cellulose chain axis).

A comparison between heats of adsorption and liquefaction allows us to roughly evaluate the nature of the interactions occurring during adsorption. For example, the similarity observed for adsorption enthalpy and liquefaction for benzene, xylene, and toluene (the differences are about $2-4$ kJ mol^{-1}) suggests that only weak interactions occur during the adsorption of these compounds over the cellulose surface. For the other compounds, differences observed between adsorption and condensation enthalpies ($8-26$ kJ mol^{-1}) as shown in Table 2 suggest strong interactions occur during their elution over the cellulose support. We must attribute such differences to the functional groups substituted on the aromatic ring.

Modeling. *Behavior of the Cellulose Surfaces during Dynamics.* Figure 3 represents the behavior of the acetophenone molecule in the presence of the (110) surface of cellulose, chosen here as a representative example.

In this study, we have considered two types of cellulose chains. The first concerns chains that could interact with the adsorbate molecule and are therefore unconstrained; they are allowed to adjust their conformations to take into account environmental differences due to the interface together with the interactions with the adsorbate molecule. The second is composed of chains not in contact with the adsorbate molecule; they represent the inner bulk chains of the cellulosic material chains and are constrained. Such constraints mimic conformational restrictions due to packing forces, caused by the surrounding molecules, and allow a limited number of atoms to be taken into account without affecting the realism of the modeled systems. This is illustrated in Figure 3A, which displays the 50 structures of the first molecular dynamics superimposed in a view parallel to the cellulose fiber axis. The constraints on the cellulose layer not directly interacting with the adsorbate molecule as well as the conformational disorder of the cellulose chains located at the interface can be clearly discerned. Great conformational adaptability and significant dynamics of the surface chains were observed showing that (110), (100), and amorphous surfaces are stable during the dynamics experiments whereas a strong reorganization of the chains occurs for the (010) surface.

Adsorption of Guest Molecules on Cellulose. The method to assess the preferred interaction sites of the guest molecules onto the cellulose surface can be compared to a simulated annealing protocol. Elevated temperature allows the guest molecule to quickly reach the cellulosic surface, while a lower temperature allows the guest molecule to explore the different adsorption sites.

Two distinct behaviors of the acetophenone molecule can be distinguished in Figure 3A. One, the molecule freely moves in the accessible empty space of the simulated system, and two, it adsorbs on the molecular surface of cellulose. Figure 3B shows the time evolution of the distance between the mass center of the acetophenone molecule and the average plane of the cellulose surface. The arrow indicates when the temperature is decreased. The acetophenone molecule reaches the surface in 15 ps, and it stays adsorbed for the rest of the simulation time, desorption not being observed until the end of the modeling.

A superimposition of the final 30 conformations, viewed perpendicular to the cellulose fiber axis, is shown in Figure 3C. The molecule explores only a limited area of the surface of cellulose, and many adsorption geometries are accessible. This figure also illustrates the importance of the periodic boundary conditions: if the guest molecule leaves the system by one face of the system, it re-enters by the opposed face. Therefore, the modeled surfaces can be considered as infinite, free from undesirable edge effects.
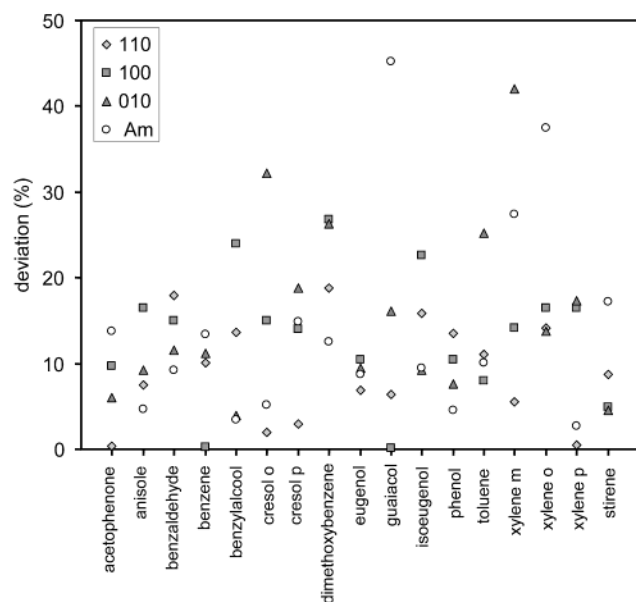
Comparison between Experimental and Predicted Adsorption Energies. *Overall Agreement.* The predicted energies between the aromatic compounds and each of the four cellulose surfaces are given in Table 3. Adsorption energies are all negative, suggesting that adsorption is favorable. For a given adsorbate molecule, the adsorption energies are of the same order of magnitude from one surface to the other, but they are surface dependent. Differences vary from 0.1 kJ/mol for benzene to 22.2 kJ/mol for dimethoxybenzene.

Figure 4 reports the deviation, expressed in %, between experimental and predicted data for each adsorbate and each surface. The agreement is globally satisfactory. Statistically, 84% of the predicted data correctly reproduce the experimental data within 20% error. Moreover, the whole predicted data set corresponding to the (110) surface is in good agreement with the experimental measurements. Adsorption energies of only three systems (adsorbate/one cellulose surface) are incorrectly predicted, and they concern the crystalline (010) or the amorphous surfaces.

Table 3. Predicted Adsorption Energies over the Surfaces of Cellulose

| | $-\Delta H_{calc}$ (kJ mol^{-1}) | | | | | |
| | cellulose surfaces | | | | averages[a] | |
adsorbate	110	100	010	Am	Av	wAv
acetophenone	59.2	53.6	55.8	51.2	55.0	55.4
anisole	53.4	48.2	52.4	60.4	53.6	54.4
benzaldehyde	70.2	68.4	66.4	65.0	67.6	67.9
benzene	33.0	36.8	40.8	31.8	35.6	34.3
benzylalcool	82.8	55.4	70.0	75.4	70.8	74.0
o-cresol	62.6	52.2	81.2	64.6	65.2	63.5
p-cresol	65.2	57.8	54.6	57.2	58.8	60.2
dimethoxybenzene	67.4	60.8	61.2	93.4	70.8	73.0
eugenol	75.2	89.2	88.4	73.8	81.6	79.0
guaiacol	68.0	63.8	74.2	92.8	74.8	75.2
isoeugenol	71.4	65.6	77.0	76.8	72.6	72.6
phenol	55.6	57.6	59.4	67.2	60.0	59.8
toluene	35.4	36.6	49.8	43.8	41.4	39.8
o-xylene	50.0	36.6	37.8	60.2	46.2	49.0
m-xylene	41.4	50.0	62.2	31.8	46.4	42.7
p-xylene	43.6	36.6	51.4	42.6	43.6	42.9
styrene	47.8	49.8	54.8	61.4	53.4	53.0

[a] The columns Av and wAv correspond to unweighted and weighted averages, respectively (see the text).

Figure 4. Graphical representation of the comparison between experimental and predicted adsorption energies.

Experimental adsorption enthalpies were obtained by assuming that no adsorbate−adsorbate interactions take place during the adsorption of aromatic compounds on cellulose. To maintain a certain coherency and realism between theoretical and experimental approaches of this study, the modeling work was carried out with a single molecule adsorbing on the cellulose surfaces. However, during the chromatographic elution, a molecule adsorbed on the column support can be desorbed by carrier gas and transported to the next interaction site. In the modeling experiment, the only driving force for adsorption of guest compounds on cellulose during the simulation is the adsorbate−adsorbent interaction. Predicted atomistic behavior is therefore based on a simplified molecular mechanism of the adsorption−desorption phenomenon taking place during the elution of a compound through a chromatographic column. Satisfactory agreement between the experimental and the corresponding simulated data suggests that modeling correctly reproduced the adsorption phenomenon.

Morphology of the Cellulosic Material. To estimate the pertinence of the considered surfaces, we have defined an

Table 4. Scale (k) and Reliability (R) Factors as a Function of Different Morphologies of Cellulose

| cellulose surfaces (%) | | | | | |
110	100	010	Am	k	R
100	0	0	0	1.03	1.3
0	100	0	0	1.1	3.14
0	0	100	0	0.98	2.91
0	0	0	100	0.97	2.57
25	25	25	25	1.02	0.97
39	28	10	23	1.03	0.87

overall agreement factor, R, defined as

$$R = \frac{\sum (\Delta H_{obs} - k\Delta H_{calc})^2}{\sum \Delta H_{obs}^2} \quad (3)$$

where

$$k = \frac{\sum \Delta H_{obs}}{\sum \Delta H_{calc}} \quad \Delta H_{calc} = \sum P_{ijk}E_{ijk} \text{ and } \sum P_{ijk} = 100$$

ΔH_{obs} corresponds to the observed adsorption enthalpy, and ΔH_{calc} to the (weighted average) predicted adsorption enthalpy. ΔH_{calc} is calculated as the sum of the predicted adsorption energies (E_{ijk}) for all surfaces, each weighted by the population of the surface (P_{ijk}). k is a factor to scale the calculated data with respect to the observed data. The smaller the value of R, the better the agreement.

Table 4 reports agreement factors and k parameters, computed for different theoretical morphologies of the cellulosic material. The scale parameter k is systematically close to unity, confirming that the order of magnitude of the predicted adsorption energies is close to the measured adsorption enthalpies.

Adsorption occurring on one of the cellulose surfaces was considered initially. This assumption implicitly considers that the adsorption is specific or that a particular surface dominates the morphology of the material and that the other surfaces are not significant or not accessible. The corresponding R factors (calculated from adsorption energies for each individual surface) range from 1.30 to 2.91. The minimum R was observed for the (110) surface which has been experimentally observed as the most abundant. R is systematically larger than 2 for the other three surfaces. According to this criterion, the (100) surface is not the most favored for the adsorption of aromatic compounds. This contrasts however with the specific adsorption of CBM on cellulose on the (100) surface through stacking interactions between aromatic residues of CBM and the exposed CH groups of glucoses. All adsorbates used in the present study have in common with CBM an aromatic ring, but their adsorption on this particular cellulose surface does not seem to be specific.

A more realistic analysis can be done by considering each cellulose surface effectively contributing to the adsorption process. The morphology of cellulose is complex, being represented by a combination of the four surfaces. If we assume that all the four surfaces have equal abundances and accessibilities, the theoretically predicted average adsorption enthalpies for each adsorbate can be calculated as the simple arithmetic average of the energies calculated for the four surfaces. For unweighted averages, general agreement is improved, compared to preceding cases. The overall agreement factor R reaches 0.97, suggesting that the "real average" surface of the cellulosic material is better described by considering all four modeled surfaces.
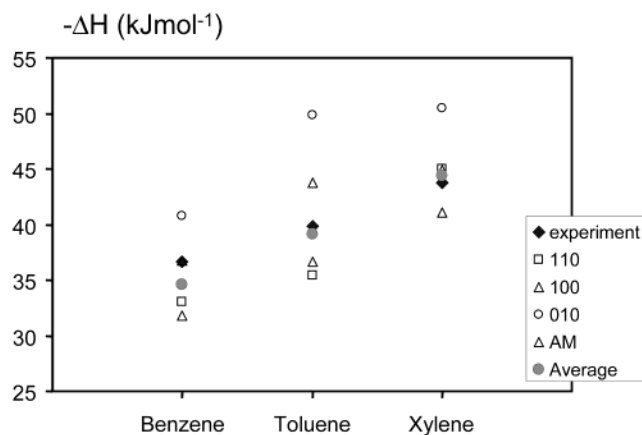
Figure 5. Adsorption enthalpies of hydrophobic molecules.

Figure 6. Group contribution to total adsorption energy; comparison between experimental and predicted data.

Experimental evidence has demonstrated that the surfaces are not equivalent in the equilibrium morphology of cellulose material. The contribution of each surface to adsorption energy is statistically related to the relative abundance of each surface. The present study allows a quantitative estimation of the relative population of each surface, by fitting the calculated data to the experimental data using the standard minimization method. The agreement factor is minimal, at 0.71, for a morphology composition represented by 39, 28, 10, and 23% for the (110), (100), (010), and amorphous surfaces, respectively. Although, to our knowledge, no precise experimental data on the surface distribution is available, the estimated relative abundance of each surface is realistic, in particular for the (110) surface, which is the most abundant according to the literature. This suggests that the surfaces used in our modeling work are pertinent and encourages us to consider all the surfaces of the cellulose material for the theoretical study of the adsorption phenomenon. We have also computed the R factor for different combinations of two and three surfaces, but R was systematically larger.

By adopting this distribution of surfaces for the morphology of microcrystalline cellulose, we could calculate the differences between experimental and the weighted average predicted adsorption enthalpies. The differences are between 0 and 5% for 7 of the 17 compounds (anisole, benzyl alcohol, *o*-cresol, eugenol, toluene, xylene, and styrene), between 6 and 10% for four other adsorbates (acetophenone, benzene, *p*-cresol, and phenol), and between 11 and 15% for the four remaining molecules (benzaldehyde, 1,2-dimethoxyphenol, guaiacol, and isoeugenol).

Group Contribution. *Monosubstituted Molecules.* The adsorption data obtained for the monosubstituted molecules allow an estimation of the contribution of each functional group to the total adsorption energies.

In Figure 5, the adsorption enthalpies of hydrophobic molecules benzene, toluene, and *p*-xylene are plotted. The experimental adsorption energy of benzene on cellulose is 36.7 kJ/mol. The average contribution of each methyl group to the adsorption enthalpy is about 3.5 kJ mol^{-1}. These results are in agreement with those reported by Gray et al.[6,7] and Dernovaya et al.,[11] but the values obtained here for aromatic compounds are slightly lower than those obtained for linear alkanes. The contribution of each methylene group to the adsorption enthalpy on cellulose varies from 5.3 to 5.6 kJ mol^{-1}, according to Gray's results. In our case, we can expect a slight decrease of this contribution due to the hindering, rigidity, and electronic density effects of the aromatic ring. However, in good agreement with previous results, a good linearity of the
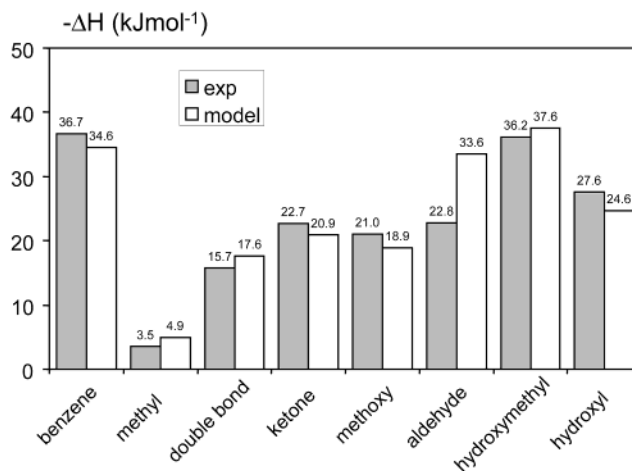
adsorption enthalpy with the number of carbon atoms is observed, suggesting a flat orientation of the molecules over the cellulose surface. The geometry of adsorption is therefore optimal, and all the functional groups effectively interact with cellulose.

The adsorption energies predicted by modeling are in the same order of magnitude as those deduced from experimental data. None of the individual surfaces is able to reproduce the experimental data, while the weighted average adsorption energies, calculated with the proportions mentioned previously, correlate very well with experimental values. The variation in the predicted adsorption energy is linear with the number of methyl groups, and their individual contribution to the total adsorption energy, 4.9 kJ/mol, is in good agreement with our experimental data and those of Gray. Furthermore, the results demonstrate that benzene, toluene, and *p*-xylene do maximize van der Waals interactions with cellulose during adsorption.

Adsorption energies are larger for the hydrophilic monosubstituted molecules than those obtained for hydrophobic molecules. This strongly suggests that favorable interactions occur between the functional groups of the adsorbates and the exposed hydroxyl groups of the cellulose surfaces. Figure 6 reports the experimental and calculated functional group contributions to the total energies. The contribution of groups acting as both donor and acceptor of hydrogen bonds, hydroxyl and hydroxymethyl, is the most important among all the substituents present in the compounds used in this work.

The concordance between experimental and theoretical values is very good (hydroxymethyl group, $\Delta H_{obs} = 36.2$ kJ mol^{-1} and $\Delta H_{calc} = 37.6$ kJ mol^{-1}; hydroxyl group, $\Delta H_{obs} = 27.6$ kJ mol^{-1} and $\Delta H_{calc} = 24.6$ kJ mol^{-1}). The second most important contribution comes from the groups possessing an oxygen acceptor of hydrogen bonds such as the carbonyl group (aldehyde and ketone) and the methoxyl group. The experimental contribution of these groups to the adsorption energy is roughly constant (about 21$-$23 kJ/mol). The predicted data are slightly underestimated by 3 kJ/mol for the ketone and methoxyl functions. However, the adsorption energy of the aldehyde group is not correctly predicted, a overestimation of 9 kJ/mol being observed when compared to the experimental data. Finally, good agreement is obtained for the group contribution of the conjugated double bond (15.7 kJ mol^{-1} experimentally and 17.6 kJ mol^{-1} theoretically).

Interaction Mechanisms of Multifunctional Molecules. The analysis of the contributions of di- and trisubstituted

Table 5. Adsorption Energies Calculated from the Group Contribution, Found Experimentally, and Predicted by Modeling for the Multisubstituted Molecules

	experimental	modeling	group contribution
o-cresol	61.4	63.5	68.3
p-cresol	67.2	60.2	
1,2-dimethoxybenzene	83.0	73.0	78.7
guaiacol	63.9	75.2	85.3
eugenol	80.8	79.0	106.7
isoeugenol	84.8	72.6	

compounds is more difficult because of the conjugation of their individual contributions, the possibility of interactions between them, and the competition of the different groups vis-à-vis the adsorption sites.

To analyze the effects of different groups on the adsorption energy of multisubstituted aromatic compounds, the experimental adsorption enthalpy, the predicted adsorption enthalpy by modeling, and the hypothetical adsorption enthalpy calculated from benzene and the individual group contributions estimated from experimental data were examined (Table 5).

For some compounds (*p*-cresol and dimethoxy-benzene), it was observed that the sum of the group contribution gives energies close to the experimental values, suggesting that these molecules adsorb flat on the surface of cellulose and all the functional groups interact with the surfaces. Therefore, the observed adsorption energies correspond to the sum of the adsorption energy of each group.

For all the other compounds, the experimentally measured energy is lower than obtained from the group contributions. This observation reveals that the interaction with the surface in this case is incomplete; the different groups do not interact with cellulose at the same time.

For the *o*-cresol molecule, for example, the experimental result suggests that one group interacts with the surface cellulose at a time. The preferred interaction must be with hydroxyl groups, but the presence of a methyl group in the *ortho* position leads to a lower adsorption energy than for phenol.

The experimental adsorption enthalpy of guaiacol (63.9 kJ mol^{-1}) is surprisingly lower than that obtained from the group contribution rule when compared to 1,2-dimethoxyphenol (85.9 kJ mol^{-1}). While the individual group contribution of each methoxyl for 1,2-dimethoxyphenol (23.1 kJ mol^{-1}) is quite close to that observed for the methoxyl-monosubstituted compound (anisol, 21 kJ mol^{-1}), the two hydrophilic groups of guaiacol only add 27 kJ mol^{-1} to the adsorption energy. These results suggest that intramolecular and intermolecular interactions are in competition for the molecules having a hydroxyl group and a methoxyl group in the *ortho* configuration, that is, guaiacol and eugenols. An intramolecular hydrogen bond can form between these two groups, leading to a gap of 20−22 kJ/mol between the experimental energy and the estimated one from group contributions.

This understanding of the adsorption process is consistent with the results obtained by molecular modeling despite significant differences between the energies predicted by modeling and those calculated from group contributions. The multifunctional molecules cannot fully interact with cellulose; in most of the cases, only a part of the adsorbed molecules is effectively "touching" the surface. Adsorption is therefore a compromise between surface roughness of cellulose and conformational adaptability of the adsorbate. It also depends on the availability of the surface hydroxyls of the cellulose material and on the configuration and conformations of the adsorbate.

Conclusions

A comparative and complementary study involving experimental determination of isosteric adsorption enthalpy and atomistic modeling of aromatic compounds over a microcrystalline cellulose surface is presented. The experimental work is derived from the Clausius−Clapeyron equation and the temperature dependence of retention volume at infinite dilution within the validity of Henry's law. Four different celluloses surfaces (110, 100, and 010 crystalline and an amorphous phase) were considered for the modeling approach.

Adsorption enthalpies of the studied compounds range from 36.7 kJ mol^{-1} for benzene to 84.8 kJ mol^{-1} for isoeugenol. The differences observed between the experimental adsorption enthalpies and the heat of liquefaction vary from 2−4 kJ mol^{-1} for hydrophobic compounds to 8−26 kJ mol^{-1} for aromatic molecules substituted with hydrophilic groups.

During the modeling of the adsorption process, two different steps were observed: first the adsorbate freely moves in the empty space available above the adsorbant before adsorbing on the cellulose surface where it stays until the end of the modeling. However, the adsorption is not static since we observed that the molecule moves along different sites of the cellulose surface.

A good correlation between experimentally measured and theoretically predicted average values, calculated as the difference between the energy of the isolated components (cellulose and aromatic molecule) and the total energy of system after adsorption, was obtained. Eighty-four percent of experimental adsorption energies are predicted with 20% of error or less. This global agreement encouraged us to propose a typical morphology of the microcrystalline cellulose, represented as a weighted combination of the four considered surfaces: 39% (110), 28% (100), 10% (010), and 23% amorphous. By considering this surface distribution, the differences between experimental adsorption enthalpies and those assessed by modeling are less than 10% for 82% of the compounds studied here.

Estimates of group contribution were carried out based on both experimental and theoretical predictions. Good agreement is obtained for most functional groups such as methyl (ΔH_{obs} = 3.5 kJ mol^{-1}, ΔH_{calc} = 4.9 kJ mol^{-1}), hydroxyl (ΔH_{obs} = 27.6 kJ mol^{-1}, ΔH_{calc} = 24.6 kJ mol^{-1}), hydroxymethyl (ΔH_{obs} = 36.2 kJ mol^{-1}, ΔH_{calc} = 37.6 kJ mol^{-1}), methoxyl (ΔH_{obs} = 21.0 kJ mol^{-1}, ΔH_{calc} = 18.9 kJ mol^{-1}), double bond (ΔH_{obs} = 15.7 kJ mol^{-1}, ΔH_{calc} = 17.6 kJ mol^{-1}), and ketone (ΔH_{obs} = 22.7 kJ mol^{-1}, ΔH_{calc} = 20.9 kJ mol^{-1}) but underestimated for the aldehyde group (ΔH_{obs} = 33.6 kJ mol^{-1} and ΔH_{calc} = 22.8 kJ mol^{-1}). The adsorption of multisubstituted aromatic compounds depends on the possibilities of simultaneous interactions of the functional groups, which is governed by a compromise between the roughness of the cellulose surface and the conformational adaptability of the compound.

The work described provides new opportunities to improve the understanding of the interaction details of multifunctional aromatic molecules and cellulose at the atomic scale.